

Food & Function

Accepted Manuscript



This is an *Accepted Manuscript*, which has been through the Royal Society of Chemistry peer review process and has been accepted for publication.

Accepted Manuscripts are published online shortly after acceptance, before technical editing, formatting and proof reading. Using this free service, authors can make their results available to the community, in citable form, before we publish the edited article. We will replace this *Accepted Manuscript* with the edited and formatted *Advance Article* as soon as it is available.

You can find more information about *Accepted Manuscripts* in the [Information for Authors](#).

Please note that technical editing may introduce minor changes to the text and/or graphics, which may alter content. The journal's standard [Terms & Conditions](#) and the [Ethical guidelines](#) still apply. In no event shall the Royal Society of Chemistry be held responsible for any errors or omissions in this *Accepted Manuscript* or any consequences arising from the use of any information it contains.

20 **ABSTRACT**

21 Phytochemical profiles and bioactivities of red, white and pink globe amaranth
22 (*Gomphrena haageana* K., *Gomphrena globosa* var. *albiflora* and *Gomphrena* sp.,
23 respectively), much less studied than the purple species (*G. globosa* L.), were
24 compared. The chemical characterization of the samples included the analysis of
25 macronutrients and individual profiles in sugars, organic acids, fatty acids, tocopherols,
26 and phenolic compounds. Their bioactivity was evaluated by determining the
27 antioxidant and anti-inflammatory activities; the absence of cytotoxicity was also
28 determined. Red and pink samples showed the highest sugars content. Otherwise, the
29 white sample gave the highest level of organic acids, and together with the pink one
30 showed the highest tocopherol and PUFA levels. Quercetin-3-*O*-rutinoside was the
31 major flavonol in white and pink samples, whereas a tetrahydroxy-
32 methylenedioxyflavone was the major compound in the red variety, which revealed a
33 different phenolic profile. Pink globe amaranth hydromethanolic extract revealed the
34 highest antioxidant activity, followed by those of red and white samples. The anti-
35 inflammatory activity was more relevant in red and pink varieties. None of the samples
36 presented toxicity in liver cells. Overall, these samples can be used in bioactive
37 formulations against inflammatory processes and free radicals production.

38

39 **Keywords:** *Gomphrena* species; Nutritional composition; Phenolic compounds;
40 Antioxidant activity; Anti-inflammatory activity

41

42 **1. Introduction**

43 Medicinal plants play a vital role on the health and healing of man, not only in
44 traditional medicine but also as one of the major sources of drugs.¹ Plants synthesize a
45 variety of secondary metabolites, many of which are bioactive and could have
46 commercial interest as pharmaceutical compounds, being capable to protect and treat
47 against various diseases.² Recently, there has been an increasing interest in the
48 therapeutic potential of plants as antioxidants, reducing free radicals that induce tissue
49 injury, and as anti-inflammatories. Although several synthetic drugs are commercially
50 available, their safety and toxicity is a concern, so there is a tendency to substitute them
51 by natural compounds.³

52 Oxidative stress and inflammation play critical roles in the pathogenesis of many
53 diseases, such as cancer, cardiovascular disease, arthritis or obesity.⁴ Oxidative stress
54 occurs when the balance between pro-oxidants and antioxidants is disturbed, resulting
55 in tissue accumulation of free radicals and other reactive oxygen species (ROS). If the
56 human body does not eliminate these harmful products, they may cause oxidative
57 damage to functional macromolecules such as DNA, proteins and lipids.⁵ Inflammation
58 is one of the body's self-defense systems that are classified as part of our innate
59 immunity. Thus, bacterial or viral infections trigger numerous immunological events,
60 including the production of cytokines, chemokines, and inflammatory mediators such as
61 nitric oxide (NO), prostaglandin E2 (PGE2) or tumor necrosis factor (TNF)- α ,^{6,7} whose
62 activation is mediated by the nuclear factor-kappa B (NF- κ B), a transcription factor that
63 regulate the transcription of DNA,⁸ as well as the migration and infiltration of
64 leukocytes, the increased expression of surface molecules such as MHC (Major
65 Histocompatibility Complex) molecules, complement receptors, and the release of
66 hydrolytic enzymes.⁹

67 Bioactive molecules such as phenolic compounds, quinones, vitamins, coumarins, and
68 alkaloids, are present in a large number of plants species.¹⁰ Phenolic compounds are the
69 most numerous and ubiquitously distributed groups of plant secondary metabolites,
70 presenting a wide range of biological effects mainly related to their antioxidant capacity
71 due to the presence of H-donating hydroxyl groups.¹¹ It is also strongly suggested in the
72 literature that plant polyphenols inhibit the inflammation process by regulating the
73 production of pro-inflammatory molecules, such as TNF- α ,¹² leukocyte adhesion, and
74 NO, all produced during inflammatory reactions.^{13,14} Inflammatory pathways
75 simultaneously contribute to and are regulated by oxidative stress. In fact, NO reacts
76 with free radicals, such as superoxide, to produce highly damaging peroxynitrites,
77 which can oxidize low-density lipoproteins that lead to irreversible damage in cell
78 membranes. Hence, inhibition of production of such pro-inflammatory molecules (NO
79 and TNF- α) is expected to have therapeutic value as antioxidant agents and against
80 inflammatory diseases.^{13,15}

81 *Gomphrena sp.* is a comestible and commercial ornamental plant commonly known as
82 globe amaranth or bachelor button that belongs to the family *Amaranthaceae*.¹⁶ Plants
83 of this family are particularly predominant in South America, consisting of
84 approximately 120 species, which are employed in folk medicine in the treatment of
85 several diseases due to their biological activities, including antimicrobial,¹⁷ antioxidant,
86 cytotoxic,¹⁸ hypotensive activities,¹⁹ and that also possess nutritive value.²⁰

87 Recent studies have focused mainly on the most common cultivar, purple globe
88 amaranth, dealing with its phytochemical composition,^{20,21} antimicrobial, antioxidant
89 and cytotoxic activities, and cardiovascular effects,^{18,22,23} as well as its medicinal
90 benefits.²⁴ Nevertheless, at the best of our knowledge, other *Gomphrena* species are still
91 poorly or non-studied and, since the consumption data indicate that these plants are

92 widely employed around the world for various purposes, especially their traditionally
93 used as infusions in order to treat throat disorders, hence it seems of great interest to
94 explore their bioactive potential.

95 Therefore, the aim of this study was to compare the phytochemical profile and bioactive
96 properties of different varieties of globe amaranth (red, white and pink), and contribute
97 to the characterization of the less studied *Gomphrena* species.

98

99 **2. Material and Methods**

100 **2.1. Samples**

101 Three different cultivars (red, white and pink) of *Gomphrena* species, commonly known
102 as globe amaranth, were obtained from “Cantinho das Aromáticas”, organic farmers
103 from Vila Nova de Gaia (Portugal), as dry flower material (supplementary material).
104 Red, white and pink dried flowers samples corresponded to *Gomphrena haageana* K.,
105 *Gomphrena globosa* var. *albiflora* and *Gomphrena* sp., respectively.

106

107 **2.2. Standards and reagents**

108 Acetonitrile 99.9%, *n*-hexane 95% and ethyl acetate 99.8% were of HPLC grade from
109 Fisher Scientific (Lisbon, Portugal). Fatty acids methyl ester (FAME) reference
110 standard mixture 37 (standard 47885-U) was purchased from Sigma (St. Louis, MO,
111 USA), as also were other individual fatty acid isomers, trolox (6-hydroxy-2,5,7,8-
112 tetramethylchroman-2-carboxylic acid), L-ascorbic acid, tocopherol, sugar and organic
113 acid standards. Racemic tocol, 50 mg/mL, was purchased from Matreya (Pleasant Gap,
114 PA, USA). Phenolic standards were from Extrasynthèse (Genay, France). 2,2-Diphenyl-
115 1-picrylhydrazyl (DPPH) was obtained from Alfa Aesar (Ward Hill, MA, USA).
116 Dulbecco’s modified Eagle’s medium, hank’s balanced salt solution (HBSS), fetal

117 bovine serum (FBS), L-glutamine, trypsin-EDTA, penicillin/streptomycin solution (100
118 U/mL and 100 mg/ mL, respectively) were purchased from Gibco Invitrogen Life
119 Technologies (Paisley, UK). Sulforhodamine B, trypan blue, trichloro acetic acid (TCA)
120 and Tris were purchased from Sigma Chemical Co. (Saint Louis, MO, USA).
121 RAW264.7 cells were purchased from ECACC (“European Collection of Animal Cell
122 Culture”) (Salisbury, UK), lipopolysaccharide (LPS) from Sigma and DMEM medium
123 from HyClone. The Griess Reagent System Kit was purchased from Promega, and
124 dexamethasone from Sigma. Water was treated in a Milli-Q water purification system
125 (TGI Pure Water Systems, Greenville, SC, USA).

126

127 **2.3. Nutritional composition**

128 **2.3.1. Nutritional value**

129 The samples were analyzed for chemical composition (protein, fat, carbohydrates and
130 ash) using the AOAC procedures.²⁵ The crude protein content of the samples (N×6.25)
131 was estimated by the macro-Kjeldahl method; the crude fat was determined using a
132 Soxhlet apparatus by extracting a known weight of sample with petroleum ether; the ash
133 content was determined by incineration at 600±15 °C. Total carbohydrates were
134 calculated by difference and total energy was calculated according to the following
135 equation: Energy (kcal) = 4 × (g protein + g carbohydrates) + 9 × (g fat).

136

137 **2.3.2. Sugars**

138 Free sugars were determined via high performance liquid chromatography coupled to a
139 refraction index detector (HPLC-RI), after an extraction procedure previously described
140 by the authors²⁶ using melezitose as internal standard (IS). The equipment consisted of
141 an integrated system with a pump (Knauer, Smartline system 1000, Berlin, Germany),
142 degasser system (Smartline manager 5000), auto-sampler (AS-2057 Jasco, Easton, MD,

143 USA) and an RI detector (Knauer Smartline 2300). Data were analyzed using Clarity
144 2.4 Software (DataApex, Prague, Czech Republic). The chromatographic separation
145 was achieved with a Eurospher 100-5 NH₂ (Knauer) column (5 μm, 4.6 × 250 mm)
146 operating at 35 °C (7971 R Grace oven). The mobile phase was acetonitrile/deionized
147 water, 70:30 (v/v) at a flow rate of 1 mL/min. The compounds were identified by
148 chromatographic comparisons with authentic standards. Quantification was performed
149 using the internal standard method and sugar contents were further expressed in g per
150 100 g of dry weight.

151

152 **2.3.3. Organic acids**

153 Organic acids were determined following a procedure previously described by the
154 authors.²⁷ The analysis was performed using a Shimadzu 20A series UFLC (Shimadzu
155 Corporation, Kyoto, Japan). Separation was achieved on a SphereClone (Phenomenex,
156 Torrance, CA, USA) reverse phase C₁₈ column (5 μm, 4.6 × 250 mm) thermostatted at
157 35 °C. The elution was performed with sulphuric acid 3.6 mM using a flow rate of 0.8
158 mL/min. Detection was carried out in a PDA, using 215 nm and 245 nm (for ascorbic
159 acid) as preferred wavelengths. The organic acids found were quantified by comparison
160 of the area of their peaks with calibration curves obtained from commercial standards of
161 each compound. For quantitative analysis, calibration curves were prepared from
162 different standard compounds: oxalic acid ($y=10^7x+96178$; $R^2=0.999$); malic acid
163 ($y=952269x+17803$; $R^2=1$); fumaric acid ($y=172760x+52193$; $R^2=0.999$). The results
164 were expressed in g per 100 g of dry weight.

165

166 **2.3.4. Tocopherols**

167 Tocopherols were determined following a procedure previously described by the
168 authors.²⁶ Analysis was performed by HPLC (equipment described above), and a
169 fluorescence detector (FP-2020; Jasco) programmed for excitation at 290 nm and
170 emission at 330 nm. The chromatographic separation was achieved with a Polyamide II
171 (YMC Waters, Milford, MA, USA) normal-phase column (5 μm , 4.6 mm \times 250 mm),
172 operating at 35 $^{\circ}\text{C}$. The mobile phase used was a mixture of *n*-hexane and ethyl acetate
173 (70:30, *v/v*) at a flow rate of 1 mL/min. The compounds were identified via
174 chromatographic comparisons with authentic standards. Quantification was based on the
175 fluorescence signal response of each standard, using the IS (tocol) method and by using
176 calibration curves obtained from commercial standards of each compound. The results
177 were expressed in mg per 100 g of dry weight.

178

179 **2.3.5. Fatty acids**

180 Fatty acids were determined by gas-liquid chromatography with flame ionization
181 detection (GC-FID)/capillary column as described previously by the authors.²⁶ The
182 analysis was carried out with a DANI model GC 1000 instrument equipped with a
183 split/splitless injector, a flame ionization detector (FID at 260 $^{\circ}\text{C}$) and a Macherey–
184 Nagel column (30 m \times 0.32 mm i.d. \times 0.25 μm df, Bethlehem, PA, USA). The oven
185 temperature program was as follows: the initial temperature of the column was 50 $^{\circ}\text{C}$,
186 held for 2 min, then a 30 $^{\circ}\text{C}/\text{min}$ ramp to 125 $^{\circ}\text{C}$, 5 $^{\circ}\text{C}/\text{min}$ ramp to 160 $^{\circ}\text{C}$, 20 $^{\circ}\text{C}/\text{min}$
187 ramp to 180 $^{\circ}\text{C}$, 3 $^{\circ}\text{C}/\text{min}$ ramp to 200 $^{\circ}\text{C}$, 20 $^{\circ}\text{C}/\text{min}$ ramp to 220 $^{\circ}\text{C}$ and held for 15
188 min. The carrier gas (hydrogen) flow-rate was 4.0 mL/min (0.61 bar), measured at 50
189 $^{\circ}\text{C}$. Split injection (1:40) was carried out at 250 $^{\circ}\text{C}$. Fatty acid identification was made
190 by comparing the relative retention times of FAME peaks from samples with standards.

191 The results were recorded and processed using the CSW 1.7 Software (DataApex 1.7,
192 Prague, Czech Republic) and expressed in relative percentage of each fatty acid.

193

194 **2.4. Non-nutrients composition**

195 ***2.4.1. Extraction procedure***

196 The dry material was used to prepare hydromethanolic extracts by adding 25 mL of
197 methanol:water (80:20 v/v) to 1 g of each sample. The extraction was carried out by
198 stirring at 150 rpm for 1 h and subsequently filtering through Whatman No. 4 paper.
199 The residue was then extracted with an additional 25 mL of methanol:water (80:20 v/v)
200 for another hour in the same conditions. The combined extracts were evaporated at 40
201 °C in a rotary evaporator (Büchi R-210, Flawil, Switzerland), frozen and lyophilized
202 (FreeZone 4.5, Labconco, Kansas City, MO, USA).

203

204 ***2.4.2. Analysis of phenolic compounds***

205 The previously described hydromethanolic extracts were dissolved in water:methanol
206 (80:20, v/v) to a final concentration of 20 mg/mL and analysed using a Hewlett-Packard
207 1100 chromatograph (Hewlett-Packard 1100, Agilent Technologies, Santa Clara, CA,
208 USA) with a quaternary pump and a diode array detector (DAD) coupled to an HP
209 Chem Station (rev. A.05.04) data-processing station. A Waters Spherisorb S3 ODS-2
210 C₁₈, (3 µm, 4.6 mm × 150 mm) column thermostatted at 35 °C was used. The solvents
211 used were: (A) 0.1% formic acid in water, (B) acetonitrile. The elution gradient
212 established was isocratic 15% for 5 min, 15% B to 20% B over 5 min, 20-25% B over
213 10 min, 25-35% B over 10 min, 35-50% for 10 min, and re-equilibration of the column,
214 using a flow rate of 0.5 mL/min. Double online detection was carried out in the DAD

215 using 280 nm and 370 nm as preferred wavelengths and in a mass spectrometer (MS)
216 connected to HPLC system via the DAD cell outlet.²¹

217 MS detection was performed in an API 3200 Qtrap (Applied Biosystems, Darmstadt,
218 Germany) equipped with an ESI source and a triple quadrupole-ion trap mass analyser
219 that was controlled by the Analyst 5.1 software. Zero grade air served as the nebulizer
220 gas (30 psi) and turbo gas for solvent drying (400 °C, 40 psi). Nitrogen served as the
221 curtain (20 psi) and collision gas (medium). The quadrupols were set at unit resolution.
222 The ion spray voltage was set at -4500V in the negative mode. The MS detector was
223 programmed for recording in two consecutive modes: Enhanced MS (EMS) and
224 enhanced product ion (EPI) analysis. EMS was employed to show full scan spectra, so
225 as to obtain an overview of all of the ions in sample. Settings used were: declustering
226 potential (DP) -450 V, entrance potential (EP) -6 V, collision energy (CE) -10V. EPI
227 mode was performed in order to obtain the fragmentation pattern of the parent ion(s) in
228 the previous scan using the following parameters: DP -50 V, EP -6 V, CE -25V, and
229 collision energy spread (CES) 0 V. Spectra were recorded in negative ion mode between
230 m/z 100 and 1500.

231 The phenolic compounds were identified by comparing their retention time, UV-vis and
232 mass spectra with those obtained from standard compounds, when available. Otherwise,
233 peaks were tentatively identified from the information obtained from their mass spectra
234 and data reported in the literature. For quantitative analysis, a calibration curve for each
235 available phenolic standard was constructed based on the UV signal: *p*-coumaric
236 ($y=884.6x+184.49$; $R^2=0.999$); kaempferol-3-*O*-glucoside ($y=288.55x-4.0503$; $R^2=1$);
237 kaempferol-3-*O*-rutinoside ($y=239.16x-10.587$; $R^2=1$); isorhamnetin-3-*O*-glucoside
238 ($y=218.26x-0.98$; $R^2=1$); isorhamnetin-3-*O*-rutinoside ($y=284.12x+67.055$; $R^2=0.999$);
239 quercetin-3-*O*-glucoside ($y=363.45x+117.86$; $R^2=0.999$), quercetin-3-*O*-rutinoside

240 $(y=281.98x-0.3459; R^2=1)$. For the detected phenolic compounds for which a
241 commercial standard was not available, the quantification was performed through the
242 calibration curve of other compound from the same phenolic group. The results were
243 expressed in mg per g of lyophilized extract.

244

245 **2.5. Antioxidant activity evaluation**

246 For the antioxidant activity assays, the lyophilized hydromethanolic extracts were
247 dissolved in methanol:water (80:20 v/v) and concentrated at 10 mg/mL. For the different
248 assays, these extracts were then submitted to further dilutions from 10 mg/mL to 0.02
249 mg/mL.

250 DPPH radical-scavenging activity was evaluated by using an ELX800 microplate reader
251 (Bio-Tek Instruments, Inc; Winooski, VT, USA), and calculated as a percentage of
252 DPPH discolouration using the formula: $[(A_{DPPH}-A_S)/A_{DPPH}] \times 100$, where A_S is the
253 absorbance of the solution containing the sample at 515 nm, and A_{DPPH} is the
254 absorbance of the DPPH solution. Reducing power was evaluated by the capacity to
255 convert Fe^{3+} into Fe^{2+} , measuring the absorbance at 690 nm in the microplate reader
256 mentioned above. Inhibition of β -carotene bleaching was evaluated through the β -
257 carotene/linoleate assay; the neutralization of linoleate free radicals avoids β -carotene
258 bleaching, which is measured by the formula: $(\beta\text{-carotene absorbance after 2h of}$
259 $\text{assay/initial absorbance}) \times 100$. Lipid peroxidation inhibition in porcine (*Sus scrofa*)
260 brain homogenates was evaluated by the decreasing in thiobarbituric acid reactive
261 substances (TBARS); the colour intensity of the malondialdehyde-thiobarbituric acid
262 (MDA-TBA) was measured by its absorbance at 532 nm; the inhibition ratio (%) was
263 calculated using the following formula: $[(A - B)/A] \times 100\%$, where A and B were the
264 absorbance of the control and the sample solution, respectively.²¹ The results were

265 expressed in EC₅₀ values (sample concentration providing 50% of antioxidant activity
266 or 0.5 of absorbance in the reducing power assay). Trolox was used as positive control.

267

268 **2.6. Anti-inflammatory activity evaluation**

269 **2.6.1. Cells treatment**

270 For the anti-inflammatory activity assay, the lyophilized hydromethanolic extracts were
271 dissolved in water, and concentrated at 8 mg/mL. For the different assays, the extracts
272 were then submitted to further dilutions from 8 mg/mL to 0.125 mg/mL.

273 The mouse macrophage-like cell line RAW264.7 was cultured in DMEM medium
274 supplemented with 10% heat-inactivated foetal bovine serum, 100 U/mL penicillin and
275 100 mg/mL streptomycin and were incubated at 37 °C in a humidified atmosphere
276 containing 5% CO₂. For each experiment, cells were detached with a cell scraper. Under
277 our experiment cell density (5 x 10⁵ cells/mL), the proportion of dead cells was less
278 than 1%, according to Trypan blue dye exclusion tests.

279 Cells were seeded in 96-well plates at 150.000 cells/well and allowed to attach to the
280 plate overnight. Then, cells were treated with the different concentrations of each of the
281 extracts for 1h. Dexamethasone (50 µM) was used as a positive control for the
282 experiment. The following step was stimulation with LPS (1 µg/mL) for 18h. The effect
283 of all the tested samples in the absence of LPS was also evaluated, in order to observe if
284 they induced changes in NO basal levels. In negative controls, no LPS was added. Both
285 extracts and LPS were dissolved in supplemented DMEM.

286

287 **2.6.2. Nitric oxide determination**

288 For the determination of nitric oxide, Griess Reagent System kit (Promega) was used,
289 which contains sulfanilamide, NED and nitrite solutions. A reference curve of the nitrite

290 was prepared in a 96-well plate as described in the instructions thereof. One hundred
291 microliters of the cell culture supernatant was transferred to the plate in duplicate and
292 mixed with sulfanilamide and NED solutions, 5-10 minutes each, at room temperature.
293 The nitrite produced was determined by measuring the optical density at 515 nm, in the
294 microplate reader referred above, and compared to the standard calibration curve.

295

296 **2.7. Hepatotoxicity evaluation**

297 The effect of the samples on the growth of porcine liver primary cells (PLP2),
298 established by the group, was evaluated by the sulforhodamine B (SRB) colorimetric
299 assay with some modifications as described by Abreu *et al.*²⁸ Briefly, the liver tissues
300 were rinsed in Hank's balanced salt solution containing 100 U/mL penicillin and 100
301 µg/mL streptomycin and divided into 1×1 mm³ explants. Some of these explants were
302 placed in 25 cm³ tissue flasks in DMEM supplemented with 10% fetal bovine serum, 2
303 mM nonessential amino acids and 100 U/mL penicillin, 100 mg/mL streptomycin and
304 incubated at 37 °C with a humidified atmosphere containing 5% CO₂. The medium was
305 changed every 2 days. Cultivation of the cells was continued with direct monitoring
306 every 2-3 days using a phase contrast microscope. Before confluence, cells were sub-
307 cultured and plated in 96-well plates at a density of 1.0×10⁴ cells/well, and cultivated in
308 DMEM medium with 10% FBS, 100 U/mL penicillin and 100 µg/mL streptomycin.
309 Cells were treated for 48 h with the different diluted sample solutions and the SRB
310 assay was performed. The results were expressed in GI₅₀ values (sample concentration
311 that inhibited 50% of the net cell growth). Ellipticine was used as positive control.

312

313 **2.8. Statistical analysis**

314 For all the experiments, three samples were analyzed and all the assays were carried out
315 in triplicate. The results are expressed as mean values \pm standard deviation (SD). The
316 differences between the different samples were analyzed using one-way analysis of
317 variance (ANOVA) followed by Tukey's honestly significant difference post hoc test
318 with $\alpha = 0.05$, coupled with Welch's statistic. This analysis was carried out using the
319 SPSS v. 22.0 program.

320

321 **3. Results and Discussion**

322 **3.1. Nutritional composition**

323 The results obtained for macronutrients are presented in **Table 1**. Carbohydrates were
324 the major macronutrients found in all the samples (85.6 to 88.2 g/100 g), with slightly
325 higher amounts in red and white globe amaranth, followed by ash and protein. Pink
326 globe amaranth contained the highest levels of ash (7.5 g/100 g) and fat (1.20 g/100 g)
327 whereas red and white globe amaranth showed a slightly higher energy (381 and 380
328 kcal/100 g, respectively), in agreement with their higher levels of carbohydrates.

329 The chemical composition of the samples in hydrophilic (sugars and organic acids) and
330 lipophilic (fatty acids and tocopherols) compounds is shown in **Table 1**. Fructose,
331 glucose and sucrose were found in all the samples, with red and pink globe amaranth
332 revealing higher total sugars contents (2.47 and 2.40 g/100 g, respectively). The levels
333 of individual sugars were similar in the three samples, with fructose being slightly more
334 abundant in red globe amaranth (0.76 g/100 g) and glucose in pink globe amaranth
335 (1.66 g/100 g). In a recent study carried out by Pereira *et al.*,²⁹ the infusions obtained
336 from these same samples of *Gomphrena* showed carbohydrates concentrations below
337 the detection limit, which could be explained by the low levels present in the original
338 plant material.

339 Regarding organic acids, white globe amaranth revealed the highest total amount (1.32
340 g/100 g), with a significant contribution of oxalic acid (1.16 g/100 g), which was also
341 the prevailing organic acid in the other samples; red globe amaranth presented higher
342 concentration of malic acid (0.20 g/100 g) and also revealed to possess fumaric acid,
343 although in very low concentration (0.007 g/100 g).

344 Regarding tocopherols, white and pink globe amaranth showed similar levels of γ -
345 tocopherol (1.04 and 1.09 mg/100 g) and total tocopherols (1.37 and 1.38 mg/100 g,
346 respectively). α -Tocopherol was found in higher concentrations in red globe amaranth
347 (0.55 mg/100 g) that was the only sample where δ -tocopherol was not detected.

348 Up to 20 fatty acids were identified in the studied samples, with prevalence of saturated
349 fatty acids (SFA) and polyunsaturated fatty acids (PUFA) over monounsaturated fatty
350 acids (MUFA). Red globe amaranth revealed the highest percentages of SFA (58.5%),
351 with the main contribution of palmitic (C16:0; 34.6%) and stearic (C18:0; 8.1%) acids.
352 MUFA were predominant in pink globe amaranth (8.2%) that presented oleic (C18:1n9;
353 7.1%) and eicosenoic (C20:1; 0.30%) acids, whereas PUFA prevailed in white (45.9%)
354 and pink (45.6%) amaranth due to the significant contributions of linoleic (C18:2n6;
355 31.9 and 30.2%, respectively) and α -linolenic (C18:3n3; 13.7 and 15.07%, respectively)
356 acids.

357

358 **3.2. Composition in phenolic compounds**

359 Data (retention time, λ_{\max} in the visible region, pseudomolecular ion and main
360 fragment ions observed in MS²) obtained by HPLC-DAD-ESI/MS regarding phenolic
361 compounds identification and quantification in the analyzed samples of globe amaranth
362 are presented in **Tables 2** and **3**. As an example, the profile of phenolic compounds in
363 pink globe amaranth is shown in **Figure 1**.

364 The same twenty phenolic compounds, all of them flavonoid glycosides, were detected
365 in both pink (*Gomphrena* sp.) and white (*Gomphrena globosa* var. *albiflora*) globe
366 amaranth, fourteen of which had been already reported in inflorescences of purple globe
367 amaranth (*Gomphrena globosa* L.) previously analyzed in our laboratory,²¹ so that the
368 same identities have been assumed. The remaining six compounds (i.e., 1, 5, 8, 15, 16
369 and 17 in **Table 2**) have been assigned based on their mass spectral characteristics.
370 Contrary to purple globe amaranth, no hydroxycinnamoyl derivatives have been found
371 in the samples of white and pink globe amaranth now studied.
372 Compound 1 presented a pseudomolecular ion $[M-H]^-$ at m/z 741 releasing fragments at
373 m/z 609 ($[M-H-132]^-$, loss of a pentosyl moiety) and 301 (quercetin; further loss of a
374 deoxyhexosylhexoside residue, -308 mu). Although these data do not inform about the
375 nature and substitution position of the sugar moieties, compound 1 was tentatively
376 identified as quercetin 3-*O*-(2-pentosyl, 6-*O*-rhamnosyl)-hexoside owing to the previous
377 identification of such compound in inflorescences of *G. globosa* by Ferreres *et al.*³⁰
378 Compound 5 showed a pseudomolecular ion $[M-H]^-$ at m/z 593 yielding an MS²
379 fragment at m/z 285 (kaempferol) from the loss of a deoxyhexosylhexoside residue. The
380 compound is excluded to be kaempferol 3-*O*-rutinoside, which corresponds to peak 9,
381 as confirmed by comparison with a commercial standard. Buschi & Pomilio³¹ in another
382 *Gomphrena* species (*G. martiana*) reported the presence of flavonol 3-*O*-rabinosides,
383 whereas Ferreres *et al.* (2011) detected a similar compound in *G. globosa* that identified
384 as kaempferol 3-*O*-(6-rhamnosyl)-hexoside based on mass spectra, without indicating
385 the nature of the hexose. Since no support to the type of sugar substituent can be
386 concluded from the HPLC-DAD-MS analysis performed herein, the same identity as
387 suggested by Ferreres *et al.* (2011) was assumed for compound 5. Compound 8 was
388 associated to a quercetin *O*-acetylhexoside according to its pseudomolecular ion $[M-H]^-$

389 at m/z 505 and MS² fragment released at m/z 301 ([M-H-42-162]⁻, loss of acetyl and
390 hexosyl moieties). Compound 15 ([M-H]⁻ at m/z 563) could correspond to a kaempferol
391 derivative bearing pentosyl and rhamnosyl moieties. Only one MS² fragment at m/z 285
392 resulting from the loss of a disaccharide was produced, suggesting that both sugars are
393 located on the same position of the aglycone. Therefore, this compound was tentatively
394 assigned as kaempferol *O*-rhamnosyl-pentoside. As far as we know, none of these
395 compounds have been previously identified by in *G. globosa*.

396 Compounds 16 and 17 ([M-H]⁻ at m/z 607 and 649 mu, respectively) originated a base
397 peak at m/z 313 mu, which could correspond to gomphrenol (3,5,4'-trihydroxy-6,7-
398 methylenedioxyflavone) early described in *G. globosa* leaves.³² Peaks with the same
399 pseudomolecular ions were detected in *G. globosa* inflorescences by Ferreres *et al.*³⁰
400 and Silva *et al.*²⁰ and suggested to correspond to gomphrenol 3-*O*-(2-pentosyl)-hexoside
401 and gomphrenol 3-*O*-(2-pentosyl, 6 acetyl)-hexoside; so, these identities were also
402 tentatively assumed for the compounds detected in our samples. Flavonoids bearing a
403 methylenedioxy group, like gomphrenol (3,5,4'-trihydroxy-6,7-
404 methylenedioxyflavonol), are rare in nature, with a predominance in the genus
405 *Gomphrena*.³³

406 Red globe amaranth (*Gomphrena haageana* K.) presented a different phenolic profile
407 (**Table 3**) when compared with white and pink samples. Fourteen phenolic compounds
408 were detected, from which only two coincided with those observed in the other two
409 *Gomphrena* species, namely quercetin 3-*O*-rutinoside (compound 4') and quercetin 3-
410 *O*-glucoside (compound 6'). Both flavonols, as well as compound 3' (*p*-coumaric acid)
411 were positively identified by comparison with commercial standards, being also
412 previously reported in other globe amaranth varieties.^{20,21,30}

413 Compounds 1' ([M-H]⁻ at *m/z* 799) and 2' ([M-H]⁻ at *m/z* 653) would correspond to
414 isorhamnetin derivatives (λ_{max} around 354 nm and common MS² fragment at *m/z* 315)
415 bearing different number of sugar substituents. No information about the identity of the
416 sugar moieties and location onto the aglycone could be obtained, although the fact that
417 only one MS² fragment was released in both cases suggested that sugars are attached to
418 a unique position in the form of oligosaccharides. Thus, according to their molecular
419 masses they were assigned as isorhamnetin *O*-glucuronyl-deoxyhexosyl-hexoside and
420 isorhamnetin *O*-glucuronyl-hexoside, respectively.

421 Compounds 5' ([M-H]⁻ at *m/z* 639) and 7' ([M-H]⁻ at *m/z* 493) released a main MS²
422 fragment at *m/z* 331 from the loss of deoxyhexosyl-hexoside (308 mu) and hexoside
423 (162 mu) moieties, respectively. The ion at *m/z* 331 would fit patuletin, whose presence
424 reported in other species of the genus *Gomphrena*.³³ Thus, the compounds were
425 tentatively identified as patuletin *O*-deoxyhexosyl-hexoside and patuletin *O*-hexoside,
426 respectively. This latter might correspond to patuletin 3-*O*-glucoside described in *G.*
427 *claussenii* Moq. by Ferreira & Dias.³³

428 Compounds 9'-14' have been assigned as possible methylenedioxyflavonol derivatives,
429 based on their mass spectra and the previous description of similar derivatives in
430 inflorescences of *G. globosa* by Ferreres *et al.*³⁰ Compound 13' showed a
431 pseudomolecular ion [M-H]⁻ at *m/z* 491 that released an MS² fragment at *m/z* 329 (-162
432 mu; loss of a hexosyl residue), which was assumed to correspond to the deprotonated
433 aglycone matching the structure of a tetrahydroxymethylenedioxyflavone. It was
434 tentatively identified as 3,5,3',4'-tetrahydroxy-6,7-methylenedioxyflavone-3-*O*-
435 hexoside, as previously described by Ferreres *et al.*³⁰ Similarly, compound 10' ([M-H]⁻
436 at *m/z* 637) releasing a unique MS² fragment at *m/z* 329 (-308 mu) should correspond to
437 the equivalent deoxyhexosyl-hexoside derivative. Compound 9' with an ion [M-H]⁻ at

438 m/z 681 releasing fragments at m/z 343 (-338 mu; loss of glucuronyl + hexosyl residues)
439 and 328 (-15 mu; further loss of a methyl residue) might correspond to a methoxy-
440 trihydroxymethylenedioxyflavone *O*-glucuronylhexoside. Compound 11' ($[M-H]^-$ at m/z
441 767) presented a molecular mass 86 mu higher than compound 9' and the same MS²
442 fragments at m/z 343 and 328, together with another fragment at m/z 723 (- 44 mu;
443 possible loss of a CO₂ group). These characteristics pointed out to a malonyl derivative
444 of compound 9'. Compound 12' must also be related to compound 9' owing to the
445 observation of the MS² fragments at m/z 681, 343 and 328, as well as by the existence
446 of similar UV absorption spectra; however, no final structure could be drawn. No
447 identity could be assigned to compound 14', either, although the presence of a fragment
448 at m/z 328 also suggested that it may also be related to compound 9', thus also
449 belonging to the group of methylenedioxyflavones. But for compound 13', reported by
450 Ferreres *et al.*,³⁰ none of the previous compounds have been described in *G. globosa*, as
451 far as we are aware.

452 Lastly, minor compound 8' presented a MS² fragmentation pattern and UV spectrum
453 that did not allow a tentative identification of its structure.

454 Quercetin 3-*O*-rutinoside (compound 3) was the major flavonol found in white and pink
455 globe amaranth (**Table 2**), followed by kaempferol 3-*O*-rutinoside (compound 9), which
456 was also previously reported by us to be the main flavonoid the purple variety. As for
457 red globe amaranth, the majority compound was compound 10', a tetrahydroxy-
458 methylenedioxyflavone (**Table 3**). To our knowledge, this is the first report about the
459 phenolic composition of red, white and pink species of globe amaranth.

460

461 **3.3. Antioxidant activity**

462 The results of the antioxidant activity, based on radicals scavenging and lipid
463 peroxidation inhibition capacities of the hydromethanolic extracts obtained for red,
464 white and pink globe amaranth are presented in **Table 4**. Among the three studied
465 samples, pink globe amaranth showed the highest antioxidant activity, with the lowest
466 EC₅₀ values in all assays (0.25 to 1.02 mg/mL), followed by red (0.41 to 1.30 mg/mL)
467 and white (0.57 to 1.47 mg/mL) globe amaranth. The best results of antioxidant activity
468 were obtained in the TBARS assay, where the extracts revealed lipid peroxidation
469 inhibition activity in the lowest concentrations (EC₅₀ between 0.25 and 0.57 mg/mL).

470 To the best of our knowledge, there are no studies regarding the antioxidant activity of
471 the cultivars studied in the present work, although there are a couple of reports on
472 methanolic extracts²¹ and infusions²⁰ of purple globe amaranth, also from Portugal but
473 from different distributors. Regarding to DPPH scavenging activity of the infusions,
474 Silva *et al.*²⁰ reported EC₅₀ values of 0.47 mg/mL, whereas the methanolic extract
475 studied by Roriz *et al.*²¹ showed lower antioxidant activity (1.47 to 4.87 mg/mL) than
476 that achieved with the hydromethanolic extracts of the samples studied in the present
477 work (0.25 to 1.47 mg/mL).

478

479 **3.4. Anti-inflammatory activity and hepatotoxicity**

480 In the course of screening of natural products to find novel anti-inflammatory drugs, the
481 capacity of red, white and pink globe amaranth to inhibit the NO release from
482 macrophages was also tested. As shown in **Figure 2**, the hydromethanolic extracts of
483 the samples revealed a dose-dependent anti-inflammatory activity in the range of
484 concentrations checked (up to 400 µg/mL), with a considerable decrease of NO
485 production even at the low concentrated extracts. Pink and red globe amaranth showed
486 the lowest EC₅₀ values (133 and 136 µg/mL, respectively), with white globe amaranth

487 revealing a slight higher activity (198 $\mu\text{g/mL}$). The extracts lack toxicity when tested in
488 the PLP2 cell line (established as primary cultures from pig liver), even at the highest
489 concentration studied (400 $\mu\text{g/mL}$) (**Table 4**). As far as we know, this is the first report
490 on anti-inflammatory properties of these *Gomphrena* species cultivars and, from the
491 results obtained, they should be considered as potential anti-inflammatory medicines.

492

493 **4. Conclusion**

494 Overall, the phytochemical profile and bioactive properties of different cultivars of
495 globe amaranth (red, white and pink) have been compared, so as to contribute to the
496 characterization of these less studied *Gomphrena* species. To the best of authors'
497 knowledge, this is the first detailed chemical study in the mentioned varieties and data
498 obtained highlight them as sources of bioactive compounds that could be incorporated
499 in functional beverages or foods, as also in other formulations, owing to their anti-
500 inflammatory potential and valuable properties related with oxidative stress.

501

502 **Acknowledgements**

503 The authors are grateful to Foundation for Science and Technology (FCT, Portugal) for
504 financial support to the research center CIMO (strategic project PEst-
505 OE/AGR/UI0690/2014), R. Calhelha grant (SFRH/BPD/68344/2010) and L. Barros
506 researcher contract under "Programa Compromisso com Ciência – 2008".

507

508 **References**

- 509 1 S. Upadhyaya and L. R. Saikia, *Int. J. Phar. Biol. Sci.*, 2011, **2**, 383-388.
510 2 P. P. Joy, J. Thomas, S. Mathew and B. P. Skaria, *Medicinal Plants. Tropical*
511 *Horticulture Vol. 2.* (Eds. Bose, TK Kabir, J Das P and patel PP), Naya Prokash,
512 Calcutta, 2001, pp. 449-632.

- 513 3 V. R. Patel, P. R. Patel and S. S. Kajal, *Adv. Biol. Res.*, 2010, **4**, 23-26.
- 514 4 F. Sesti, O. E. Tsitsilonis, A. Kotsinas and I. P. Trougako, *In Vivo*, 2012, **26**,
515 395-402.
- 516 5 M. Carocho and I. C. F. R. Ferreira, *Food Chem. Toxicol.*, 2013, **51**, 15-25.
- 517 6 R. W. Kinne, R. Brauer, B. Stuhlmuller, E. Palombo-Kinne and G. R.
518 Burmester, *Arthritis Res.*, 2000, **2**, 189-202.
- 519 7 T. Owens, A. A. Babcock, J. M. Millward and H. Toft-Hansen, *Brain Res. Rev.*,
520 2005, **48**, 178-184.
- 521 8 P. P. Tak and G. S. Firestein, *J. Clin. Invest.*, 2001, **107**, 7-11.
- 522 9 L. Deban, B. Bottazzi, C. Garlanda, Y. M. de la Torre and A. Mantovani,
523 *Biofactors*, 2009, **35**, 138-145.
- 524 10 Y. Cai, Q. Luo, M. Sun and H. Corke, *Life Sci.*, 2004, **74**, 2157-2184.
- 525 11 A. L. Dawidowicz and M. Olszowy, *Talanta*, 2012, **97**, 312-317.
- 526 12 J. H. Yoon and S. J. Baek, *Yonsei Med. J.*, 2005, **46**, 585.
- 527 13 Y. S. Lee, O. K. Han, C. W. Park, C. H. Yang, T. W. Jeon, W. K. Yoo, S. H.
528 Kim and H.J. Kim, *J. Ethnopharmacol.*, 2005, **100**, 289-294.
- 529 14 M. Feldmann and S. Maini, *Immunol. Rev.*, 2008, **223**, 7-19.
- 530 15 C. Wang, G. B. Schuller Levis, E. B. Lee, W. R. Levis, D. W. Lee, B. S. Kim, S.
531 Y. Park and E. Park, *Int. Immunopharmacol.*, 2004, **4**, 1039-1049.
- 532 16 M. Ilyas, A. Tarnam and N. Begun, *Global J. Pharmacol.*, 2013, **7**, 457-464.
- 533 17 A. B. Pomilio, C. A. Buschi, C. N. Tomes and A. A. Viale, *J. Ehnopharmacol.*,
534 1992, **36**, 155-161.
- 535 18 M. D. Hamiduzzaman and A. T. M. Z. Azam, *Bangladesh Pharm. J.*, 2012, **15**,
536 183-185.
- 537 19 J. C. Siqueira, *Acta Biol. Leopold.*, 1987, **9**, 5-22.

- 538 20 L. R. Silva, P. Valentão, J. Faria, F. Ferreres, C. Sousa, A. Gil-Izquierdo, B. R.
539 Pinho, P. B. Andrade, *Food Chem.*, 2012, **135**, 756-763.
- 540 21 C. L. Roriz, L. Barros, A. M. Carvalho, C. Santos-Buelga, and I. C. F. R.
541 Ferreira, *Food Res. Int.*, 2014, **62**, 684-693.
- 542 22 D. D. R. Arcanjo, A. C. M. Albuquerque, B. M. Neto, L. C. L. R. Santana, N. C.
543 B. Silva, M. M. Moita, M. G. F. Medeiros, M. J. S. Soares and A. M. G. L. Citó,
544 *J. Med. Plants Res.*, 2011, **5**, 2006-2010.
- 545 23 M. D. Hamiduzzaman, A. Dey, M. M. Hossain and A. T. M. Z. Azom,
546 Investigation of biological properties of *Gomphrena globosa* (L.), Family:
547 Amaranthaceae. *J. Pharm. Res.*, 2012, **5**, 4230-4232.
- 548 24 A. H. M. M. Rahman and M. I. A. Gulshana, *Appl. Ecol. Env. Sci.*, 2014, **2**, 54-
549 59.
- 550 25 AOAC. (2012). Official methods of analysis of AOAC INTERNATIONAL.
551 (19th ed.). Gaithersburg, MD, USA: AOAC INTERNATIONAL.
- 552 26 L. Barros, E. Pereira, R. C. Calhelha, M. Duenas, A. M. Carvalho, C. Santos-
553 Buelga and I. C. F. R. Ferreira, *J. Funct. Foods*, 2013, **5**, 1732-1740.
- 554 27 C. Pereira, L. Barros, A. M. Carvalho and I. C. F. R. Ferreira, *Food Anal.*
555 *Method.*, 2013, **6**, 1337-1344.
- 556 28 R. M. V. Abreu, I. C. F. R. Ferreira, R. C. Calhelha, R. T. Lima, M. H.
557 Vasconcelos, F. Adegas, R. Chaves and M. J. R. P. Queiroz, *Eur. J. Med. Chem.*,
558 2011, **46**, 5800-5806.
- 559 29 C. Pereira, L. Barros and I. C. F. R. Ferreira, *Plant Food. Hum. Nutr.*, 2015, **70**,
560 176-183.
- 561 30 F. Ferreres, A. Gil-Izquierdo, P. Valentão and P. B. Andrade, *Rapid Commun.*
562 *Mass Spectrom.*, **25**, 3441-3446.

- 563 31 C. A. Buschi and A. B. Pomilio, *J. Nat. Prod.*, 1982, **45**, 557-559.
- 564 32 M. L. Bouillant, P. Redolfi, A. Cantisani and J. Chopin, *Phytochemistry*, 1978,
565 **17**, 2138-2140.
- 566 33 E. O. Ferreira and D. A. Dias, *Biochem. Syst. Ecol.*, 2004, **32**, 823-827.

Figure Legends

Figure 1. Phenolic profile of pink globe amaranth variety recorded at 370 nm.

Figure 2. Anti-inflammatory effect of three globe amaranth varieties (red, white and pink) hydromethanolic extracts. Levels of NO production determined by Griess assay from culture supernatants of RAW264.7 cells treated with LPS (1 $\mu\text{g}/\text{mL}$) for 24h.

Table 1. Nutritional value and nutrients in the globe amaranth cultivars.

	Red	White	Pink
Ash (g/100 g dw)	5.4 ± 0.2 ^c	6.1 ± 0.3 ^b	7.5 ± 0.4 ^a
Protein (g/100 g dw)	5.9 ± 0.3 ^a	5.6 ± 0.2 ^a	5.70 ± 0.01 ^a
Fat (g/100 g dw)	0.50 ± 0.03 ^c	0.80 ± 0.02 ^b	1.20 ± 0.06 ^a
Carbohydrates (g/100 g dw)	88.2 ± 0.3 ^a	87.5 ± 0.3 ^a	85.6 ± 0.2 ^b
Energy (kcal/100 g dw)	381 ± 1 ^a	380 ± 1 ^a	376 ± 1 ^b
Fructose (g/100 g dw)	0.76 ± 0.01 ^a	0.53 ± 0.03 ^b	0.57 ± 0.02 ^b
Glucose (g/100 g dw)	1.58 ± 0.04 ^{ab}	1.52 ± 0.07 ^b	1.66 ± 0.09 ^a
Sucrose (g/100 g dw)	0.13 ± 0.02 ^b	0.17 ± 0.01 ^a	0.17 ± 0.03 ^a
Total sugars (g/100 g dw)	2.47 ± 0.06 ^a	2.22 ± 0.04 ^b	2.40 ± 0.04 ^a
Oxalic acid (g/100 g dw)	0.82 ± 0.01 ^c	1.16 ± 0.01 ^a	0.95 ± 0.02 ^b
Malic acid (g/100 g dw)	0.20 ± 0.01 ^a	0.16 ± 0.03 ^b	0.14 ± 0.01 ^c
Fumaric acid (g/100 g dw)	0.0070 ± 0.0002	nd	nd
Total organic acids (g/100 g dw)	1.03 ± 0.02 ^c	1.32 ± 0.01 ^a	1.09 ± 0.01 ^b
α-Tocopherol (mg/100 g dw)	0.55 ± 0.03 ^a	0.28 ± 0.02 ^b	0.23 ± 0.01 ^c
γ-Tocopherol (mg/100 g dw)	0.50 ± 0.04 ^b	1.04 ± 0.06 ^a	1.09 ± 0.05 ^a
δ-Tocopherol (mg/100 g dw)	nd	0.05 ± 0.01	0.06 ± 0.01
Total tocopherols (mg/100 g dw)	1.05 ± 0.07 ^b	1.37 ± 0.08 ^a	1.38 ± 0.03 ^a
C16:0 (Palmitic acid; %)	34.6 ± 0.4	25.7 ± 0.4	25.3 ± 0.1
C18:0 (Stearic acid; %)	8.1 ± 0.1	5.93 ± 0.09	4.65 ± 0.02
C18:1n9 (Oleic acid; %)	5.38 ± 0.02	4.91 ± 0.09	7.1 ± 0.3
C18:2n6 (Linoleic acid; %)	23.6 ± 0.3	31.9 ± 0.3	30.2 ± 0.2
C18:3n3 (α-Linolenic acid; %)	10.8 ± 0.9	13.7 ± 0.8	15.07 ± 0.05
C22:0 (Behenic acid; %)	3.94 ± 0.02	5.65 ± 0.02	5.08 ± 0.03
SFA (%)	58.5 ± 0.5 ^a	48.9 ± 0.5 ^b	46.1 ± 0.4 ^c
MUFA (%)	6.0 ± 0.1 ^b	5.2 ± 0.1 ^c	8.2 ± 0.3 ^a
PUFA (%)	35.5 ± 0.5 ^b	45.9 ± 0.6 ^a	45.6 ± 0.1 ^a

dw- dry weight; nd- not detected. SFA – Saturated fatty acids; MUFA – Monounsaturated fatty acids; PUFA – Polyunsaturated fatty acids. Only the fatty acids with abundance higher than 5% were presented in the table; the difference to 100% corresponds to other fourteen less abundant fatty acids. In each row different letters mean statistically significant differences (p<0.05).

Table 2. Retention time (Rt), wavelengths of maximum absorption in the visible region (λ_{\max}), mass spectral data, identification and quantification of phenolic compounds in white and pink globe amaranth (mean \pm SD).

Peak	Rt (min)	λ_{\max} (nm)	Molecular ion [M-H] ⁻ (m/z)	Main MS ² fragments (m/z)	Tentative identification	Quantification (mg/g extract)	
						White	Pink
1	16.7	354	741	609(8),301(40)	Quercetin 3- <i>O</i> -(2-pentosyl, 6-rhamnosyl)-hexoside	0.12 \pm 0.01	0.12 \pm 0.01
2	17.9	354	595	301(100)	Quercetin 3- <i>O</i> -(6-pentosyl)-hexoside	0.12 \pm 0.01	0.15 \pm 0.01
3	18.8	354	609	301(100)	Quercetin 3- <i>O</i> -rutinoside	5.21 \pm 0.01	4.93 \pm 0.10
4	19.1	340	725	593(10),285(40)	Kaempferol 3- <i>O</i> -(2-pentosyl, 6- <i>O</i> -rhamnosyl)-hexoside	0.92 \pm 0.03	1.22 \pm 0.05
5	19.7	356	593	285(100)	Kaempferol 3- <i>O</i> -(6-rhamnosyl)-hexoside	0.36 \pm 0.01	0.44 \pm 0.02
6	20.2	356	463	301(100)	Quercetin 3- <i>O</i> -glucoside	0.71 \pm 0.01	0.73 \pm 0.02
7	21.1	352	579	447(10),285(35)	Kaempferol 3- <i>O</i> -(2-pentosyl)-hexoside	0.20 \pm 0.01	0.22 \pm 0.01
8	21.6	358	505	301(100)	Quercetin <i>O</i> -acetylhexoside	tr	0.018 \pm 0.003
9	22.3	350	593	285(100)	Kaempferol 3- <i>O</i> -rutinoside	3.27 \pm 0.03	3.31 \pm 0.01
10	23.3	352	623	315(100)	Isorhamnetin 3- <i>O</i> -rutinoside	0.71 \pm 0.02	0.75 \pm 0.01
11	23.9	350	447	285(100)	Kaempferol 3- <i>O</i> -glucoside	0.47 \pm 0.02	0.52 \pm 0.02
12	24.9	358	477	315(100)	Isorhamnetin 3- <i>O</i> -glucoside	0.31 \pm 0.01	0.36 \pm 0.03
13	26.0	346	477	315(100)	Isorhamnetin <i>O</i> -hexoside	0.39 \pm 0.01	0.39 \pm 0.01
14	26.7	346	489	285(100)	Kaempferol <i>O</i> -acetylhexoside	0.25 \pm 0.01	0.29 \pm 0.01
15	28.5	340	563	285(100)	Kaempferol <i>O</i> -rhamnosyl-pentoside	0.15 \pm 0.01	0.19 \pm 0.01
16	29.3	276,340	607	313(100)	Gomphrenol 3- <i>O</i> -(2-pentosyl)-hexoside	0.32 \pm 0.01	0.36 \pm 0.03
17	30.7	280,334	649	313(100)	Gomphrenol 3- <i>O</i> -(2-pentosyl, 6 acetyl)-hexoside	0.21 \pm 0.01	0.31 \pm 0.03
18	31.8	338	639	463(39),301(30)	Quercetin <i>O</i> -glucuronide- <i>O</i> -hexoside	0.037 \pm 0.001	0.08 \pm 0.01
19	32.3	278,342	475	313(100)	Gomphrenol 3- <i>O</i> -hexoside	0.39 \pm 0.01	0.40 \pm 0.01
20	33.9	276,340	517	313(100)	Gomphrenol 3- <i>O</i> -(6-acetyl)-hexoside	0.84 \pm 0.03	0.84 \pm 0.01
Total phenolic compounds						14.99 \pm 0.14	15.62 \pm 0.20

Table 3. Retention time (Rt), wavelengths of maximum absorption in the visible region (λ_{\max}), mass spectral data, identification and quantification of phenolic compounds in red variety of globe amaranth (mean \pm SD).

Peak	Rt (min)	λ_{\max} (nm)	Molecular ion [M-H] ⁻ (m/z)	MS ² (m/z)	Tentative identification	Quantification (mg/g)
1'	15.1	354	799	315(100)	Isorhamnetin- <i>O</i> -glucuronyl-deoxyhexosyl-hexoside	0.25 \pm 0.00
2'	16.8	354	653	315(100)	Isorhamnetin- <i>O</i> -glucuronyl-hexoside	0.83 \pm 0.00
3'	17.2	312	163	119(100)	<i>p</i> -Coumaric acid	1.00 \pm 0.04
4'	18.9	356	609	301(100)	Quercetin-3- <i>O</i> -rutinoside	1.27 \pm 0.00
5'	19.4	354	639	331(36),316(16)	Patuletin <i>O</i> -deoxyhexosyl-hexoside	0.39 \pm 0.03
6'	20.2	358	463	301(100)	Quercetin-3- <i>O</i> -glucoside	0.45 \pm 0.03
7'	20.6	354	493	331(60),316(22)	Patuletin <i>O</i> -hexoside	0.45 \pm 0.00
8'	22.0	336	829	635(22),513(56),315(100),193(20)	Unknown	nq
9'	25.1	348	681	343(96),328(51)	Methoxy-trihydroxymethylenedioxyflavone <i>O</i> -glucuronyl-hexoside	1.07 \pm 0.04
10'	26.4	346	637	329(100)	3,5,3',4'-Tetrahydroxy-6,7-methylenedioxyflavone-3- <i>O</i> -deoxyhexosyl-hexoside	3.83 \pm 0.01
11'	27.2	348	767	723(79),343(98),328(48)	Malonyl derivative of compound 9	0.83 \pm 0.01
12'	28.1	342	825	681(90),343(36),328(22)	Derivative of compound 9	0.40 \pm 0.01
13'	29.0	338	491	329(56),179(3)	3,5,3',4'-Tetrahydroxy-6,7-methylenedioxyflavone-3- <i>O</i> -hexoside	0.65 \pm 0.01
14'	30.0	346	493	447(60),328(5),315(8)	Unknown methylenedioxyflavone	3.03 \pm 0.02
Total phenolic compounds						14.46 \pm 0.03

nq- not quantified

Table 4. Antioxidant and anti-inflammatory properties, and hepatotoxicity of the hydromethanolic extracts obtained from the globe amaranth cultivars.

	Red	White	Pink
Antioxidant activity (EC ₅₀ values, mg/mL)			
DPPH scavenging activity	1.19 ± 0.06b	1.36 ± 0.03a	1.02 ± 0.01c
Reducing power	0.88 ± 0.01b	1.38 ± 0.03a	0.84 ± 0.02c
β-carotene bleaching inhibition	1.30 ± 0.04b	1.47 ± 0.04a	0.98 ± 0.06c
TBARS inhibition	0.41 ± 0.01b	0.57 ± 0.01a	0.25 ± 0.03c
Anti-inflammatory activity (EC ₅₀ values, μg/mL)			
NO production	136 ± 4b	198 ± 5a	133 ± 7b
Hepatotoxicity (GI ₅₀ values, μg/mL)			
PLP2 growth inhibition	>400	>400	>400

Results of antioxidant activity are expressed in EC₅₀ values: sample concentration providing 50% of antioxidant activity or 0.5 of absorbance in the reducing power. Results of anti-inflammatory activity are expressed in EC₅₀ values: sample concentration providing 50% of inhibition in production of NO. Results of hepatotoxicity are expressed in GI₅₀ values: sample concentration providing 50% of inhibition of the net cell growth. In each row different letters mean significant differences between samples (p<0.05).

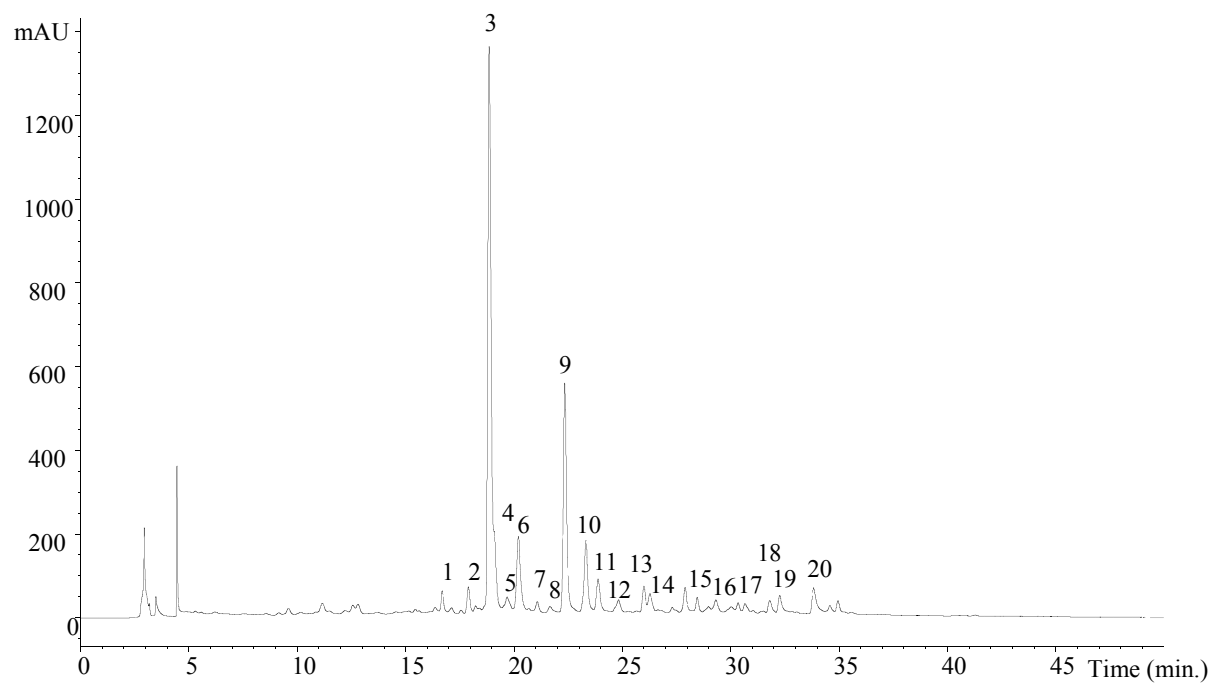


Figure 1. Phenolic profile of pink globe amaranth variety recorded at 370 nm.

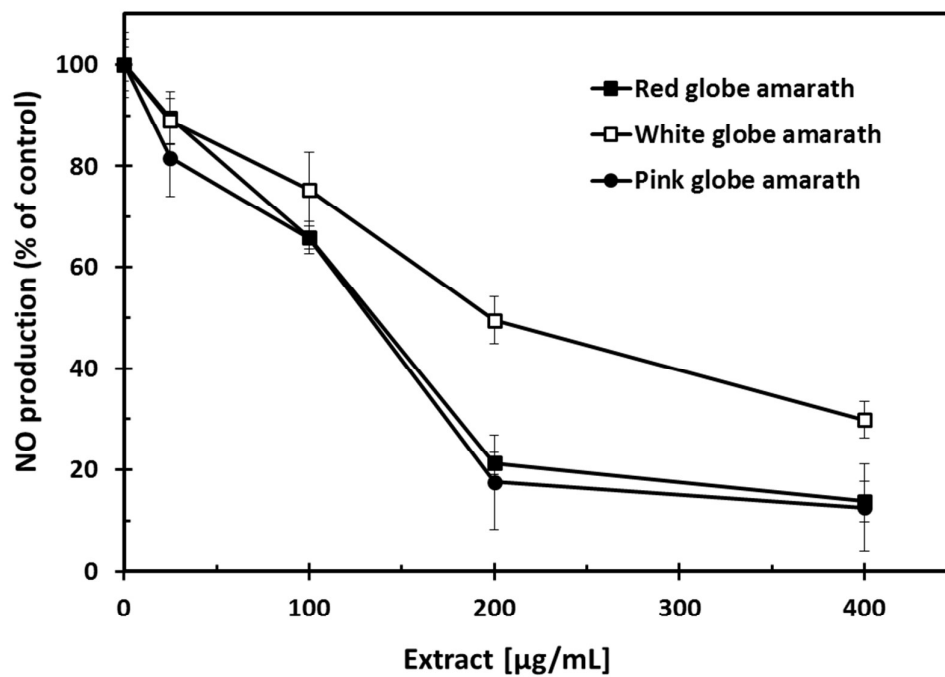


Figure 2. Anti-inflammatory effect of three globe amaranth varieties (red, white and pink) hydromethanolic extracts. Levels of NO production determined by Griess assay from culture supernatants of RAW264.7 cells treated with LPS (1 $\mu\text{g/mL}$) for 24h.

Graphical Abstract

A comparison of the bioactivity and phytochemical profile of three different cultivars of globe amaranth: red, white, and pink

Ângela Liberal, Ricardo C. Calhelha, Carla Pereira, Filomena Adegas, Lillian Barros, Montserrat Dueñas, Celestino Santos-Buelga, Rui M.V. Abreu, Isabel C.F.R. Ferreira

